ELSEVIER

Journal of Alloys and Compounds 466 (2008) 241–245

Journal of ALLOYS AND COMPOUNDS

www.elsevier.com/locate/jallcom

Spark plasma sintering and hot pressing of ZrB_2–SiC_W ultra-high temperature ceramics

Xinghong Zhang, Lin Xu *, Shanyi Du, Chengyong Liu, Jiecai Han, Wenbo Han

Center for Composite Materials and Structure, Harbin Institute of Technology, Harbin 150001, PR China

Received 26 October 2007; received in revised form 6 November 2007; accepted 7 November 2007
Available online 17 November 2007

Abstract

Zirconium diboride (ZrB_2)-based ultra-high temperature ceramics reinforced by SiC whisker were prepared by spark plasma sintering (SPS) and conventional hot pressing (HP). Dense materials were fabricated at 1600 °C by SPS and 1800 °C by HP. The densification behavior was investigated through the analysis of the HP and SPS shrinkage curves. The microstructures and mechanical properties were analyzed and compared in order to understand the influence of the two sintering techniques. The mechanical properties took full advantage of the addition of SiC whisker. Both materials exhibit high flexural strength and fracture toughness of >700 MPa and >6 $MPam^{1/2}$, respectively. The main outcome of the present work is that when the ZrB_2–SiC_W ceramics composite was densified either by SPS or HP, the mechanical properties especially fracture toughness was higher than that of analogous monolithic and composites materials.

Keywords: ZrB_2 ceramics; Microstructure; Mechanical properties

1. Introduction

Zirconium diboride (ZrB_2) and hafnium diboride (HfB_2) are members of a family of materials known as ultra-high temperature ceramics (UHTCs). Their intrinsic characteristics, i.e., high melting point, high hardness, good chemical inertness, and high wear resistance make them promising candidates for high temperature structural applications [1–4]. However, unsatisfactory values of strength and toughness are still obstacles for them to be used widely, especially for applications in severe environment. Therefore, properties must be improved before the potential applications of ZrB_2 and HfB_2 can be fully realized.

One strategy to improve the properties of monolithic materials is the addition of second phase with strengthening/toughening capabilities [5–10]. In earlier or recent studies, it was reported that SiC particle was an efficient strengthening phase for ZrB_2 and HfB_2. Chamberlain et al. [3] reported the flexural strength increased from ~550 MPa for pure ZrB_2 to ~1000 MPa for ZrB_2–20 vol.%SiCp. Likewise, fracture toughness ranged from 3.5 to 4.4 $MPam^{1/2}$ over the same composition range. The addition of SiC particle also improved oxidation resistance compared to pure ZrB_2. Unfortunately, few studies have been carried out on zirconium diboride matrix composite reinforced by SiC whisker up to date. SiC whisker, combining high strength, high elastic modulus with good thermal stability, has been successfully used to improve the properties of matrixes, such as Al_2O_3, ZrO_2, and $MoSi_2$ [9–14].

The novelty of the present contribution is that ZrB_2-based ultra-high temperature ceramics were fabricated with the reinforcement of SiC whisker by spark plasma sintering and hot pressing. Microstructure and mechanical properties were examined and discussed. The role of SiC whisker was also examined and discussed.

2. Experimental procedure

2.1. Material and processing

Commercially available raw materials were used in this study. The ZrB_2 powder with a mean size of 2 μm (>99%) was supplied from Northwest Institute for Non-ferrous Metal Research, China and the second phase used in the experiment was β-SiC whisker from Alfa Aesar, MA, USA (99%). The whisker used here has a diameter of 0.2–1.0 μm and a length of 10–50 μm. Fig. 1(a) and (b) show the morphologies of received ZrB_2 particle and SiC whisker, respectively.

* Corresponding author. Tel.: +86 45186402382; fax: +86 45186402382.
E-mail address: xulinhit@yahoo.com.cn (L. Xu).

0925-8388/$ – see front matter © 2007 Elsevier B.V. All rights reserved.
doi:10.1016/j.jallcom.2007.11.018

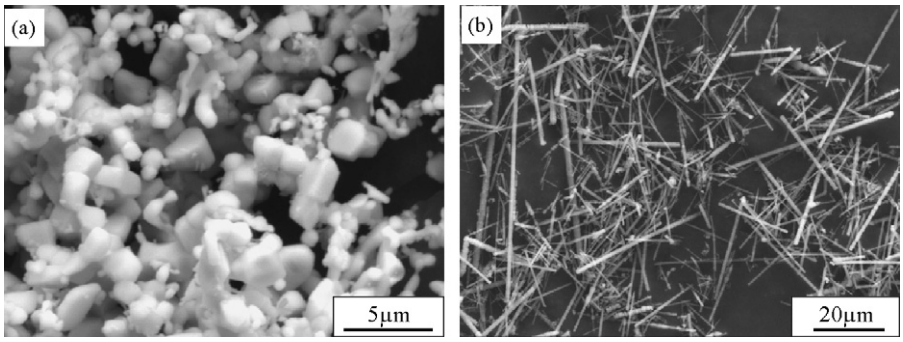

Fig. 1. Morphologies of ZrB_2 powders (a) and SiC whiskers (b).

The powder mixtures ZrB_2 plus 20 vol.% of SiC_W were ball-milled for 10 h in a polyethylene bottle using ZrO_2 balls and ethanol as the grinding media. It should be noted that the rotational speed should be restricted in 200 rpm for protecting SiC whiskers from damage (Fig. 1). After mixing, the solvent was removed by rotary evaporation to minimize segregation during drying. An amount of YAG less than 3 vol.% was introduced in both the initial powder mixtures as sintering aid.

For the spark plasma-sintering route, the powder mixture was sintered using a SPS equipment (Dr. Sinter, Model SPS-3.20MK-VI, Japan). The powder mixture was loaded into a graphite mould (inner diameter 40 mm) lined with a 0.75 mm thick graphitized paper, and pre-compacted before placed inside the SPS chamber. The sintering was carried out at 1600 °C in vacuum (<6 Pa) under a pressure of 30 MPa. The specimen was heated from room temperature to 1600 °C in 13 min by SPS, and held for 5 min, then cooled down. The temperature of the specimen was measured through the side hole of the graphite mold with an optical pyrometer (Chino IR-AHS, Japan). The difference between the actual sintering temperature and the mold surface temperature was taken into account during sintering. After completing the sintering process, the pressure was relaxed and the specimens were cooled in the chamber.

Sintering by hot pressing was carried out at 1800 °C for 60 min under a uniaxial load of 30 MPa in Ar atmosphere. The heating rate was ~15 °C/min. The sintering temperature was measured by the way of an optical pyrometer, focused on the external wall of the die. The precise heating schedule has been described elsewhere [3].

2.2. Characterization

After densification, the bulk density of hot pressed billets was determined using the Archimedes' method, while the relative density was estimated by the rule of mixture. All samples were smoothly polished using a diamond paste and ultrasonic cleaned. Phase composition was determined via X-ray diffractometry (Rigaku, Dmax-rb) using Cu-K_α radiation. The microstructure features and fractured surfaces of the composite were observed by scanning electron microscopy (SEM, FEI Sirion, Holland) with simultaneous chemical analysis by energy dispersive spectroscopy (EDS, EDAX Inc., USA). To evaluate the interface of the composites, specimens for transmission electron microscopy (TEM) were ground mechanically into 30 μm thick plate. Disc specimens of 3 mm in diameter were dimpled on one side with a Gatan dimpler, until the central region was about 10 μm thick. Final thinning to performation was carried out with a Gatan Model 600 ion-milling machine. The interface of the composite was examined in detail by JEM-2010.

Flexural strength (σ) was tested in three-point bending on 3 mm × 4 mm × 36 mm bars, using a 30 mm span and a crosshead speed of 0.5 mm/min (Instron-1186, USA). Each specimen was ground and polished with diamond slurries down to a 1 μm finish. The edges of all the specimens were chamfered to minimize the effect of stress concentration due to machining flaws. Microhardness (Hv1.0) was measured by Vickers' indentation with a

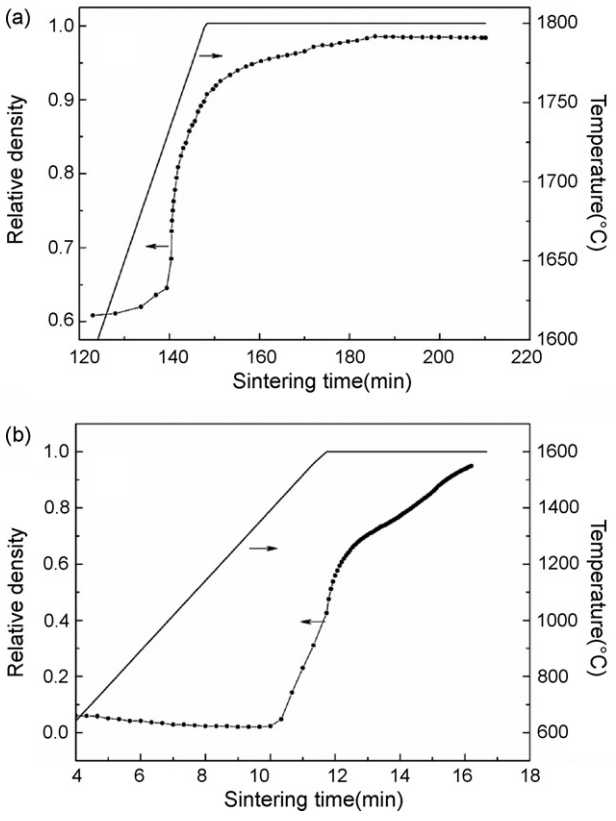

Fig. 2. Relative density (left *y*-axis) in function of sintering time for two processes: (a) hot pressing and (b) spark plasma sintering. Solid lines describe the temperature schedule (right *y*-axis).

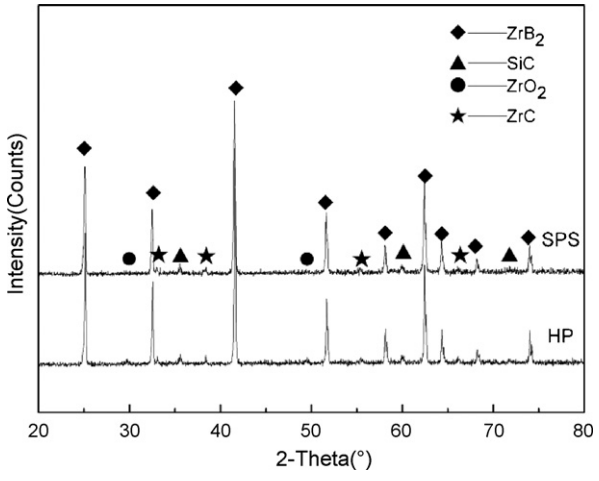

Fig. 3. XRD diffraction patterns of SPS and HP sample.

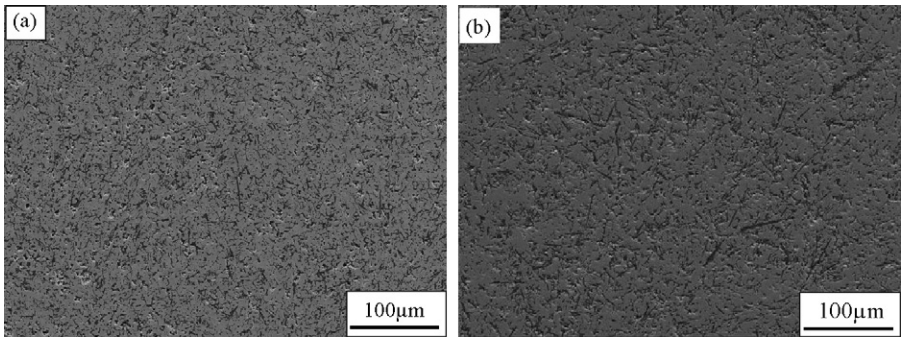

Fig. 4. SEM micrograph from a polished cross-section of the ZrB_2–SiC_W: (a) SPS and (b) HP.

9.8 N load applied for 15 s on polished sections. Fracture toughness (K_{IC}) was evaluated by a single-edge notched beam test with a 16 mm span using 2 mm × 4 mm × 22 mm test bars, on the same jig used for the flexural strength. All flexural bars were fabricated with the tensile surface perpendicular to the hot pressing direction. A minimum number of five specimens were tested for each experimental condition.

3. Results and discussion

3.1. Densification behavior

The shrinkage curves collected during spark plasma sintering and hot pressing are plotted in Fig. 2 as a function of the time, along with the temperature profile. The HP composite started to shrink at about 1670 °C and the overall duration of the thermal treatment was about 210 min. However, SPS sample (with the same composition) began to have a measurable shrinkage at around 1400 °C. That difference should be due to the different heating mode between HP and SPS. The hot pressing experiment was performed with an inductive heated device and the temperature distributions within the whole mould–specimen system were uniform. So, the measured temperature of mould can be equal as the actual temperature of sample. For comparison, high heating rates, especially in combination with short dwell times can cause temperature gradients during spark plasma sintering [15,16]. Vanmeensel et al. [17] successfully used a finite element method formalized to investigate temperature distributions during field assisted sintering technique (FAST), also known as spark plasma sintering (SPS) or pulsed electric current sintering (PECS). Result has shown that the temperature difference is ∼200 °C at a temperature of 1500 °C. In order to reduce this deflection, a pyrometer was proposed to focus on the bottom of a borehole inside the upper punch about 5 mm away from the specimen centre inside the tool [17]. During the SPS process, nearly fully dense material was obtained in less than 20 min, as shown in Fig. 2. That was probably due to the high heating rate (>100 °C/min) and the efficient heat transfer of SPS. The use of SPS technique enables the soaking time to be greatly reduced compared with hot pressing technique. However, the present of some residual porosity indicates that the spark plasma sintering conditions need to be further optimized.

3.2. Microstructural features

The X-ray diffraction analysis of sintering composites was shown in Fig. 3. ZrB_2 and β-SiC were the main phases and

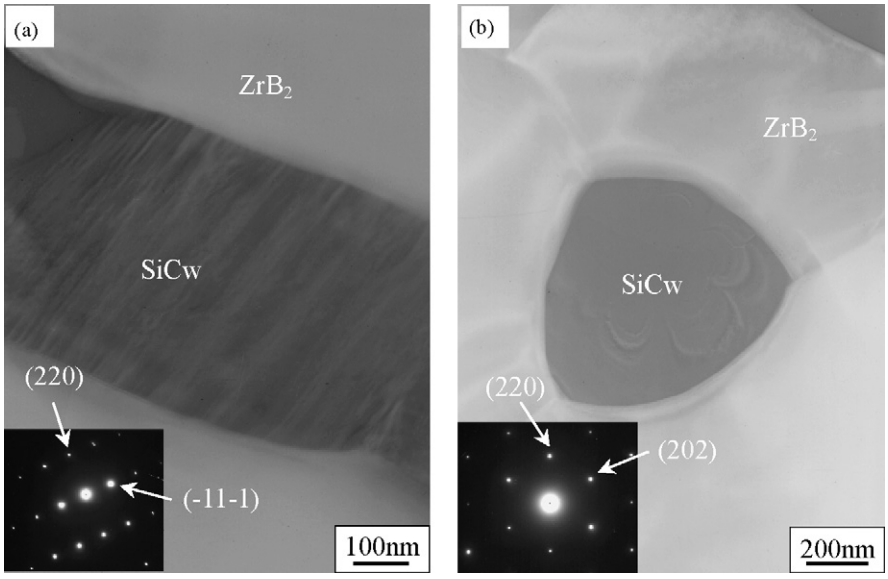

Fig. 5. TEM micrographs of interface between SiC_W and ZrB_2 in ZrB_2–SiC_W composite: (a) longitudinal section of SiC_W and (b) transverse section SiC_W.

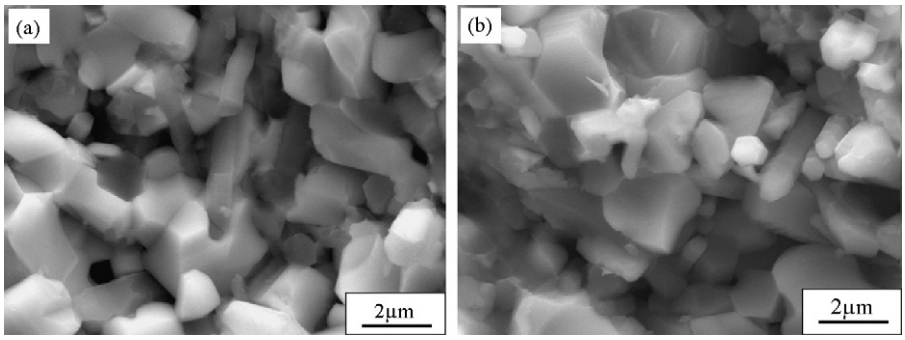

Fig. 6. SEM micrographs of the fracture surface of ZrB_2–SiC_W composites: (a) SPS and (b) HP.

some compounds in limited amounts were detected for both samples. That was presumably due to the introduction of impurities during the attrition milling and the reaction of impurities with matrix during sintering. The similar behavior has been reported for the HP or SPS ZrB_2 (HfB_2) composites [18–20]. Meanwhile, small amount of these phases such as ZrO_2 was reported to promote densification during hot pressing via introduction of liquid phases [21].

Fig. 4 shows the polished surface of SiC_W/ZrB_2 composite, revealing a uniform distribution of SiC whiskers in ZrB_2 matrix. EDS analysis (not shown here) indicated that the dark acicular phase was the SiC whisker and gray phase was ZrB_2 matrix.

Fig. 5 shows the TEM micrographs of the interface between SiC whisker and ZrB_2 in the ZrB_2–SiC_W composite after hot pressing. SiC whisker can be seen to be well bonded with the ZrB_2 matrix. The interface was clean and generally free of reaction products.

Selected-area diffraction patterns from SiC whisker are also shown in Fig. 5(a) and (b), respectively.

Fracture surfaces of SPS and HP samples are compared in Fig. 6(a) and (b), respectively. In both cases, the shape of the grains is uniform and the propagation of the fracture front involved a mixed inter/intra-granular path. Moreover, the mean ZrB_2 grain size for HP sample (~3 μm) was a little larger than the mean grain size of SPS material, ~2 μm.

3.3. Mechanical properties

The mechanical properties of the materials under investigation are listed in Table 1. The flexural strength of SPS material was slightly lower than that of HP composite. That was probably due to the lower relative density although the grain size of the latter is moderately larger than that of the former. The fracture toughness for specimens after SPS and HP was 6.02 and 6.6 $MPam^{1/2}$, respectively. The increase of the fracture toughness of HP material can be mostly explained by the increase of the flexural strength. In order to understand the strengthening effect of SiC whisker, the reported values of ZrB_2 monolithic and composites are also mentioned for comparison (Table 2). Although SPS has recently been applied to densify UHTCs [22–24], few literature data for analogous ZrB_2–SiC systems using SPS processing are available to date.

Table 1
Mechanical properties of sintered samples

Sample	Rd (%)	Sintering parameters Temperature, pressure, time	K_{IC} ($MPam^{1/2}$)	σ (MPa)
SPS	95	1600 °C, 30 MPa, 5 min	6.02 ± 0.22	708 ± 11
HP	98	1800 °C, 30 MPa, 1 h	6.60 ± 0.14	753 ± 16

Rd, relative density; K_{IC}, fracture toughness; σ, flexural strength.

The flexural strength of monolithic ZrB_2 with and without sintering aids is generally in the range of 350–565 MPa. In earlier studies, second phase such as SiC, $MoSi_2$ and ZrC was introduced to improve the densification and mechanical properties of pure material [3,5,6,18]. ZrB_2–20 vol.% SiC sintered with Si_3N_4 was reported to have higher strength of 730 MPa [18]. In a systematic study of the effect of SiC content, Chamberlain et al. [3] reported that strength increased from 565 MPa for pure ZrB_2 to 1003 MPa for ZrB_2 with 20 vol.% SiC. They are higher than other reported values. The increase in strength has been attributed to a combination of grain size reduction and the WC impurities (1.9 vol.% for ZrB_2 and 2.3 vol.% for ZrB_2–20 vol.% SiC) incorporated during attrition.

Although the strength of ZrB_2–SiCp can be improved through fine-grained and high purity starting powders, its fracture toughness is not satisfied. The reported fracture toughness ranged from 3.5 $MPam^{1/2}$ for monolithic ZrB_2 to 4.45 $MPam^{1/2}$ for ZrB_2 plus 20 vol.% SiC particle. However, in our study ZrB_2–SiC_W composites sintered by SPS or HP both exhibit higher fracture toughness (>6 $MPam^{1/2}$).

Therefore, a comparison with literature results, as mentioned above, suggests that ZrB_2–SiC_W has higher strength and toughness than monolithic ZrB_2 materials [3,18,25]. Meanwhile, the fracture toughness of SiC whisker reinforced ZrB_2 ceramic composite is much higher than earlier developed ZrB_2 composites with addition of SiC particle, as reported elsewhere [3,18,26]. To understand the toughening mechanism, the fracture surface and the path of indentation cracks was examined in the SEM. As shown in Figs. 6 and 7, the extensive crack interactions with the whisker, such as crack deflection, whisker pullout and bridging are clearly observed. It is believed that these interaction effects absorb crack propagating energy during fracture and lead to the improved toughness. The good mechanical properties of ZrB_2–SiC_W composite make it potential candidate to new style high temperature structure material.

Table 2
Reported sintering details and properties of ZrB_2 and ZrB_2–20 vol.% SiCp composites

Composition	Processing details	Rd (%)	K_{IC} (MPam$^{1/2}$)	σ (MPa)	Ref.
ZrB_2	1870 °C, 30 MPa, 30 min	90	2.3	350	[11]
ZrB_2	1900 °C, 32 MPa, 45 min	99.8	3.5	565	[3]
ZrB_2 + 4Ni	1850 °C, 30 MPa, 30 min	98.0	3.38	371	[16]
ZrB_2 + 20 vol.% SiCp	–	100	4.45	391	[17]
ZrB_2 + 20 vol.% SiCp	1900 °C, 32 MPa, 45 min	99.7	4.4	1003	[3]
ZrB_2 + 20 vol.% SiCp + 4Si_3N_4	1870 °C, 10 min	98	–	730	[11]

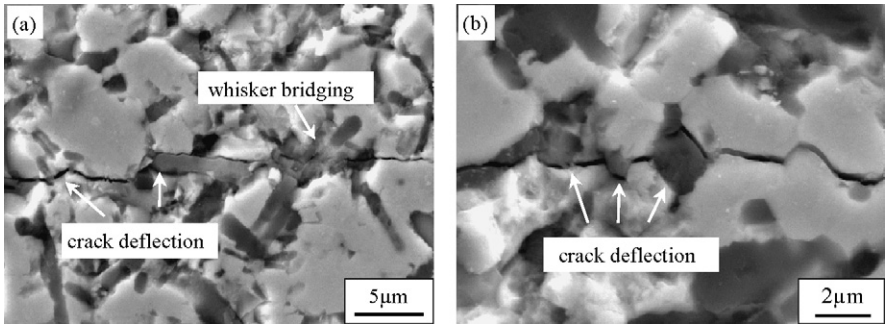

Fig. 7. SEM micrographs of indentation-induced crack propagation on a polished surface in HP ZrB_2–SiC_W composite: (a) crack deflection and whisker bridging and (b) crack deflection.

4. Conclusions

ZrB_2-based ultra-high temperature ceramics reinforced by SiC whisker were prepared by SPS and HP. The entire processing time applied to obtain nearly full dense material through spark plasma sintering was much shorter (∼20 min) than that necessary for hot pressing (∼210 min). The high effectiveness of the spark plasma sintering technique is believed to be due to the high heating rate and efficiency of the heating process.

The well-grounded property combination of this material took full advantage of the successful addition of SiC whisker. Flexural strength above 700 MPa was measured for both composites prepared by SPS and HP. The fracture toughness (>6 MPam$^{1/2}$) was much higher than that of monolithic ZrB_2 (2–3 MPam$^{1/2}$) and SiC particle reinforced ZrB_2 composite (∼4.5 MPam$^{1/2}$). The improved toughness was attributed to whisker bridging, crack deflection and whisker pullout.

Acknowledgements

This work was supported by the NSFC (90505015 and 50602010), the Research Fund for the Doctoral Program of Higher Education (20060213031).

References

[1] K. Upadhya, J.M. Yang, W.P. Hoffman, Am. Ceram. Soc. Bull. 76 (12) (1997) 51–56.
[2] S.R. Levine, E.J. Opila, M.C. Halbig, J.D. Kiser, M. Singh, J.A. Salem, J. Eur. Ceram. Soc. 22 (14) (2002) 2757–2767.
[3] A.L. Chamberlain, W.G. Fahrenholtz, G.E. Hilmas, D.T. Ellerby, J. Am. Ceram. Soc. 87 (6) (2004) 1170–1172.
[4] M.M. Opeka, I.G. Talmy, J.A. Zaykoski, J. Mater. Sci. 39 (19) (2004) 5887–5904.
[5] A.L. Chamberlain, W.G. Fahrenholtz, G.E. Gregory, D.T. Ellerby, Ceram. Trans. 153 (2004) 299–308.
[6] G.J. Zhang, M. Ando, J.F. Yang, T. Ohji, S. Kanzaki, J. Eur. Ceram. Soc. 24 (2) (2004) 171–178.
[7] F. Monteverde, Appl. Phys. A 82 (2) (2006) 329–337.
[8] F. Monteverde, A. Bellosi, Adv. Eng. Mater. 6 (5) (2004) 331–336.
[9] C.W. Li, Y. Huang, C.A. Wang, K. Tang, S.Q. Li, Q.F. Zan, Mater. Lett. 57 (2002) 336–342.
[10] P.F. Becher, G.C. Wei, J. Am. Ceram. Soc. 67 (12) (1984) c267–c269.
[11] G.Y. Lin, T.C. Lei, Y. Zhou, J. Mater. Sci. Lett. 15 (14) (1996) 1267–1270.
[12] G.Y. Lin, T.C. Lei, S.X. Wang, Y. Zhou, Ceram. Int. 22 (3) (1996) 199–205.
[13] L. Sun, J. Pan, Mater. Lett. 52 (3) (2002) 223–228.
[14] J. Deng, X. Ai, Mater. Res. Bull. 33 (4) (1998) 575–582.
[15] Y.C. Wang, Z.Y. Fu, Mater. Sci. Eng. B 90 (1–2) (2002) 34–37.
[16] A. Zavaliangos, J. Zhang, M. Krammer, J.R. Groza, Mater. Sci. Eng. A 379 (1–2) (2004) 218–228.
[17] K. Vanmeensel, A. Laptev, J. hennicke, J. Vleugels, O.V.D. Biest, Acta Mater. 53 (16) (2005) 4379–4388.
[18] F. Monteverde, S. Guicciardi, A. Bellosi, Mater. Sci. Eng. A 346 (1–2) (2003) 310–319.
[19] F. Monteverde, J. Alloy. Compd. 428 (1–2) (2007) 197–205.
[20] S.M. Zhu, W.G. Fahrenholtz, G.E. Hilmas, J. Eur. Ceram. Soc. 27 (2007) 2077–2083.
[21] S.S. Hwang, A.L. Vasiliev, N.P. Padture, Mater. Sci. Eng. A 464 (2007) 216–224.
[22] D. Sciti, L. Silvestroni, A. Bellosi, J. Mater. Res. 21 (6) (2006) 1460–1466.
[23] A. Bellosi, F. Monteverde, D. Sciti, Int. J. Appl. Ceram. Technol. 3 (1) (2006) 32–40.
[24] V. Medri, F. Monteverde, A. Balbo, A. Bellosi, Adv. Eng. Mater. 3 (2005) 159–163.
[25] F. Monteverde, A. Bellosi, S. Guicciardi, J. Eur. Ceram. Soc. 22 (3) (2002) 279–288.
[26] S.R. Levine, E.J. Opila, M.C. Halbig, J.D. Kiser, M. Singh, J.A. Salem, J. Eur. Ceram. Soc. 22 (14–15) (2002) 2757–2767.